

Spectral Analysis of a Thalamus-to-Cortex Seizure Pathway

David Lee Sherman,* *Member, IEEE*, Yien Che Tsai, Lisa Ann Rossell, Marek A. Mirski, and Nitish V. Thakor, *Fellow, IEEE*

Abstract—Physiological evidence has shown that the anterior thalamus (AN) and its associated efferents/afferents constitute an important propagation pathway for one animal model of generalized tonic-clonic epileptic seizures. In this study we extend and confirm the support for AN's role by examining neuro-electric signal indicators during seizure episodes. We show that the electroencephalogram (EEG) recorded from AN is highly coherent with the EEG derived from the cortex (CTX). By removing the effects of another thalamic nucleus, posterior thalamus (PT)—unaffiliated with the tract linking AN to cortex—partial coherence analysis leaves the CTX/AN coherence undiminished. The most robust band of strong CTX-AN coherence is centered around the spike-wave pacing frequency of 1–3 Hz. Partial-multiple coherence analysis techniques are used to remove the possible signal contributions from hippocampus in addition to PT. The CTX-AN coherence still remains undiminished in the low-frequency bands. Conclusive evidence from coherence studies and other spectral measures reaffirm the special role of the AN in the propagation of seizure activity from subcortex to cortex.

Index Terms— Coherence, EEG, epilepsy, seizure, spectrum, thalamus.

I. INTRODUCTION

THE PRECISE neuronal pathways underlying the initiation, propagation, and termination of epileptic seizure activity remains largely unknown [1]. The mechanisms underlying the creation of highly synchronized neuroelectric patterns have been studied in susceptible subcortical nuclei, such as the hippocampus [1], [2]. However, tracing the progression of seizure activity from subcortex to cortical neuronal elements is an unfamiliar and open problem. A key goal is to establish the pathways for transmission of generalized epileptic electrical discharges activating subcortical and cortical centers [3].

Seizures can be induced in experimental animals through administration of certain drugs that comprise an epilepsy model.

Manuscript received November 1, 1995; revised February 27, 1997. This work was supported by the National Institutes of Health under Grant #NS24282. The work of D. L. Sherman was supported by the Whitaker and McDonnell-Pew Foundations. The work of M. A. Mirski was supported by the American Epilepsy Society. *Asterisk indicates corresponding author.*

*D. L. Sherman is with the Department of Biomedical Engineering; Johns Hopkins School of Medicine, Johns Hopkins University, Baltimore, MD 21205 USA (e-mail: dsherman@bme.jhu.edu).

Y. C. Tsai, and N. V. Thakor are with the Department of Biomedical Engineering, Johns Hopkins School of Medicine, Johns Hopkins University, Baltimore, MD 21205 USA.

L. A. Rossell is with the Philadelphia College of Osteopathic Medicine, Philadelphia, PA 19102 USA.

M. A. Mirski is with the Queens Medical Center, Honolulu, HI 96813 USA.

Publisher Item Identifier S 0018-9294(97)05345-7.

Strong neural pathway evidence for one model of generalized tonic-clonic epilepsies exists in the case of chemically-induced pentylenetetrazol (PTZ) seizures. Mirski *et al.* have established that the thalamic anterior nuclear complex (AN), a thalamic element of the limbic system is an important gating center for the propagation of PTZ seizure activity [3]–[7]. Physiological evidence verifying the role of AN in epilepsy derived through electrical measurement during seizure episodes is lacking, though. The electroencephalogram (EEG) is the primary indicator of intense neural synchronization that occurs during epileptic activity. Coherence analysis is a technique from spectral estimation used for estimating the degree of linear association between two signals as a function of frequency.

There have been varied uses of coherence in EEG studies. The application of coherence analysis for investigating linear relationships among multichannel EEG was described by Walter and Adey [8]. Brazier [9], using coherence and phase analysis, was able to trace the spread of seizure activity in human patients. Gersch and Goddard [10] applied partial coherence to the localization of an induced epileptic focus in cat. Tharp and Gersch [11] later showed that partial coherence analysis was able to detect the appearance and migration of epileptic foci in one patient. Tucker *et al.* [12] exploit partial and partial-multiple coherence techniques in ascertaining the level of within-hemisphere association during the performance of cognitive tasks. As far as subcortical influences on cortical activity are concerned, Lopes da Silva *et al.* [13] used partial coherence analysis to check on the relative contribution of thalamic input to intracortical coherences. Using signal analysis techniques alone, Lopes da Silva achieves a “theoretical thalamic deafferentation” by removing thalamic influences from cortical associations [13].

Our study focuses on the coherence analysis to verify the hypothesis that AN has a predominant level of association with cortex during epileptic seizure activity. Our idea is to use partial coherence estimation techniques [11], [14], [15] to obtain truly independent thalamic nucleus-to-cortex coherence estimates free of cross-channel interference or contamination.

II. ANATOMICAL CONSIDERATIONS

The AN is considered a component of limbic brain that is linked to the hypothalamus and midbrain via the mammillothalamic tracts. The mammillary bodies (MB) are afferent inputs to AN. Earlier experiments by Green and Morin have shown that square wave stimulation of MB caused neural synchronization which acted as a “rhythmic pacemaker” for

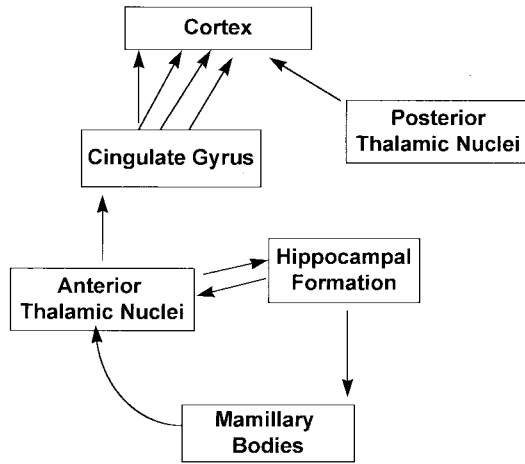


Fig. 1. Proposed schematic showing connections of circuit containing AN, HPC, and mammillary bodies to CTX. Separate channel involving PT nuclei is also depicted.

cortical activity. Under normal conditions MB and CTX did not exhibit any correlated EEG output.

Another member of the limbic system is the hippocampal (HPC) formation, which has been linked as a source for epileptic activity. AN, MB, and HPC form the “circuit of Papez,” which has direct and diffuse connections to cortex [16]. AN provides afferent input to the highly epileptogenic cingulate cortex which has diffuse cortical connections [17]. AN is the sole thalamic nucleus without major connections to reticular thalamus [18], [19]. The reticular thalamus has been cited by a number of investigators as a key center controlling cortical EEG synchronization and desynchronization. This inhibitory relay nucleus is responsible for generation of cortical EEG spindling as well.

From a communications perspective, the neuroanatomic pathways by which seizure activities spread can be modeled as a simplified network in which various brain centers interact with one another, the activity of each is reflected in the local EEG. We propose such a functional scheme in Fig. 1. The degree of interaction between two centers can, therefore, be quantified with the coherence function, which effectively measures the degree of linear association between the recorded EEG signals during different phases of an epileptic seizure expression.

III. METHODS

A. Coherence Estimation

Derivations for ordinary and partial coherence are found in Bendat and Piersol [14]. We begin with a generalization of ordinary coherence for more than two channels with consideration of multiple coherence. Partial and partial-multiple coherence follow from this perspective [20]. Since simple volume conduction of the seizure EEG through the extracellular medium can account for high CTX/AN coherences, there is a necessity for comparing CTX/AN EEG coherences with a nearby thalamic nucleus of assumed limited involvement during PTZ seizures. We wish to compare the magnitudes of thalamic nucleus to cortex coherences from AN and a nucleus

unaffiliated with the MT tract or the PT. One consideration necessitates the use of partial coherence analysis [14] in comparing CTX/AN to CTX/PT coherences. Highly correlated intrathalamic signals may result from volume conduction. Partial coherence provides some method of signal separation.

At the same time we would like to test the strong association between AN and HPC. After removing the effects of PT, we can show that the signals recorded at AN and HPC are related by removing HPC contributions from the CTX-AN partial coherence. This coherence, called the *partial-multiple coherence*, would vanish in cases where there is high correspondence between CTX or AN and HPC.

1) *Multiple Coherence*: An extension of the ordinary coherence function, the multiple coherence between a signal $y(t)$ and a set of signals $\{x(t)\}$ measures the extent to which $y(t)$ can be predicted from $\{x(t)\}$ by optimum linear least squares relationships. Consider the multiple inputs

$$\mathbf{x}(t) = [x_1(t) \cdots x_q(t)]^T \quad (1)$$

with transfer functions

$$\mathbf{H}(f) = [H_1(f) \cdots H_q(f)]. \quad (2)$$

If we denote the cross-spectra matrices by

$$\mathbf{S}_{\mathbf{x}y}(f) = [S_{1y}(f) \cdots S_{qy}(f)]^T \quad (3)$$

and

$$\mathbf{S}_{\mathbf{x}\mathbf{x}}(f) = \begin{bmatrix} S_{11}(f) & S_{12}(f) & \cdots & S_{1q}(f) \\ S_{21}(f) & S_{22}(f) & \cdots & S_{2q}(f) \\ \vdots & \vdots & \ddots & \vdots \\ S_{q1}(f) & S_{q2}(f) & \cdots & S_{qq}(f) \end{bmatrix} \quad (4)$$

where $S_{iy}(f) = S_{x_i y}(f)$ and $S_{ij}(f) = S_{x_i x_j}(f)$, the system can be described by

$$S_{yy}(f) = \mathbf{H}(f) \mathbf{S}_{\mathbf{x}\mathbf{x}}(f) \mathbf{H}^H(f) \quad (5)$$

where H stands for Hermitian transpose.

The multiple coherence between $y(t)$ and $\{x(t)\}$ is given by

$$\gamma_{y\mathbf{x}}^2(f) = 1 - \frac{|\mathbf{S}_{y\mathbf{x}\mathbf{x}}(f)|^2}{S_{yy}(f) |\mathbf{S}_{\mathbf{x}\mathbf{x}}(f)|}, \quad 0 \leq \gamma_{y\mathbf{x}}^2(f) \leq 1 \quad (6)$$

where

$$\mathbf{S}_{y\mathbf{x}\mathbf{x}}(f) = \begin{bmatrix} S_{yy}(f) & \mathbf{S}_{y\mathbf{x}}(f) \\ \mathbf{S}_{\mathbf{x}y}(f) & \mathbf{S}_{\mathbf{x}\mathbf{x}}(f) \end{bmatrix}. \quad (7)$$

It can be shown [14] that for ideal multiple input system, the multiple coherence between the output $y(t)$ and inputs $\{x(t)\}$

$$\gamma_{y\mathbf{x}}^2(f) = \frac{\sum_{i=1}^q \sum_{j=1}^q \mathbf{H}_i(f) S_{ji}(f)}{S_{yy}(f)} = 1. \quad (8)$$

We can, therefore, interpret multiple coherence as the portion of $y(t)$ that can be accounted for by an optimum linear combination of $\{x(t)\}$.

2) *Partial-Multiple Coherence*: We now generalize the concept of partial coherence to include multiple inputs ($N > 2$). Suppose we want to determine the unique relationship between $y(t)$ and one of the inputs, say $x_1(t)$. If we denote

$$\mathbf{z}(t) = [y(t), x_1(t)]^T \quad (9a)$$

and

$$\mathbf{w}(t) = [x_2(t) \cdots x_q(t)]^T \quad (9b)$$

then (13) can be rewritten as

$$\mathbf{S}_{y\mathbf{x}\mathbf{x}}(f) = \begin{bmatrix} \mathbf{S}_{zz}(f) & \mathbf{S}_{z\mathbf{w}}(f) \\ \mathbf{S}_{\mathbf{w}z}(f) & \mathbf{S}_{\mathbf{w}\mathbf{w}}(f) \end{bmatrix} \quad (10)$$

where

$$\mathbf{S}_{zz}(f) = \begin{bmatrix} S_{yy}(f) & S_{y1}(f) \\ S_{1y}(f) & S_{11}(f) \end{bmatrix} \quad (11)$$

and $\mathbf{S}_{\mathbf{w}z}(f)$ and $\mathbf{S}_{\mathbf{w}\mathbf{w}}(f)$ are cross-spectra matrices defined in similar way as (9) and (10). The conditioned spectral matrix of $\mathbf{z}(t)$ is then

$$\mathbf{S}_{z\mathbf{z}|\mathbf{w}}(f) = \mathbf{S}_{zz}(f) - \mathbf{S}_{z\mathbf{w}}(f)\mathbf{S}_{\mathbf{w}\mathbf{w}}^{-1}(f)\mathbf{S}_{\mathbf{w}z}(f) \quad (12)$$

from which the partial cross spectrum and autospectra of $y(t)$ and $x_1(t)$ after removing the linear effects of $\mathbf{w}(t)$ [26]

$$S_{1y|\mathbf{w}}(f) = S_{1y}(f) - S_{1\mathbf{w}}(f)\mathbf{S}_{\mathbf{w}\mathbf{w}}^{-1}(f)\mathbf{S}_{\mathbf{w}y}(f) \quad (13a)$$

$$S_{yy|\mathbf{w}}(f) = S_{yy}(f) - S_{y\mathbf{w}}(f)\mathbf{S}_{\mathbf{w}\mathbf{w}}^{-1}(f)\mathbf{S}_{\mathbf{w}y}(f) \quad (13b)$$

$$S_{11|\mathbf{w}}(f) = S_{11}(f) - S_{1\mathbf{w}}(f)\mathbf{S}_{\mathbf{w}\mathbf{w}}^{-1}(f)\mathbf{S}_{\mathbf{w}1}(f) \quad (13c)$$

can be obtained. The partial (multiple) coherence is then given by

$$\gamma_{1y|\mathbf{w}}^2(f) = \frac{|S_{1y|\mathbf{w}}(f)|^2}{S_{11|\mathbf{w}}(f)S_{yy|\mathbf{w}}(f)}, \quad 0 \leq \gamma_{1y|\mathbf{w}}^2 \leq 1. \quad (14)$$

An efficient algorithm for computing partial-multiple coherence is developed in Bendat and Piersol [14]. We apply partial-multiple coherence to study the relationship between cortex and AN when the effects of both PT and hippocampus are removed.

B. Experimental Methods

Male Sprague-Dawley rats ($n = 6$) purchased from Charles River, Wilmington, MA, weighing 250–300 g were anesthetized with halogen/oxygen and placed on a stereotaxic frame. All six animals had EEG recorded from AN and PT nuclei and transcortical sites. Three animals had additional depth-electrodes placed in hippocampus. Two epidural electrodes were placed behind bregma. Depth electrodes were implanted as follows: AN—1.5-mm posterior to bregma (AP), 1.5 mm lateral to midline (L) and 6.0 mm ventral to cortical surface (D); PT—4.3-mm AP, 1.5-mm L and 6.0-mm D; hippocampus—4.5-mm AP, 4.0-mm L and 2.6-mm D. Durelon liquid glue and powder were used to hold the electrodes and pedestal in place.

Animals were allowed to recover for a minimum of two days. A jugular venous catheter was placed at least 1 h prior to experiment. At least 30-s of baseline EEG were recorded before the infusion of PTZ administered at 5.5 mg/kg/min. Behavior and EEG's were continuously monitored and the extent of seizure stages were noted according to the modified clinical Racine scale [21]. All the animals passed through all stages to clonic and full clonic/tonic stages at the R-value of six. Histological follow-up confirmed the position of electrodes. Analog data was amplified with a Grass model (8-10 D) eight-channel, portable polygraph with internal 0.3-Hz highpass and 70-Hz lowpass filter cutoffs. A 60-Hz notch was also employed. The signals were recorded on analog tape using a seven-channel FM cassette data recorder (model MR-30, TEAC Corp., Japan). Analog data were digitized with CODAS (DATAQ Instruments Inc., Akron, OH) using a sampling rate of 500 Hz. Subsequent analysis was performed on signals digitally filtered with a finite impulse response (FIR) filter with 100-Hz cutoff and decimated-in-time by a factor of two, for a resulting sampling rate of 250 Hz.

C. Data Analysis

1) *Segmentation*: Digitized EEG were divided into 2-s segments for analysis. For statistical analysis, clonic episodes of EEG were chosen to have at least 8 s of sustained cortical spike-and wave activities with two spike complexes per second or greater and coincident with appropriate behavioral indicators. Two consecutive 4-s artifact-free clonic segments and two consecutive 4-s segments of artifact-free baseline EEG were extracted for comparison.

2) *Spectral Estimates*: After detrending, each 4-s segment was divided into seven 256-point overlapping segments (50% overlap) and tapered with a Hanning window. Autospectral and cross-spectral densities were estimated for each channel using fast Fourier transform (FFT) methods and averaged over segments by using the Welch overlapped segment averaging method (WOSA) [22]. To better quantify differences in power distribution among the channels, we define the band relative power as the fraction of total power contained within that band

$$\bar{P}_k = \frac{\sum_{f_i \in \text{band } k} |X_i|^2}{\sum_{f_i \in \Omega} |X_i|^2}. \quad (15)$$

3) *Coherence Estimates*: Ordinary coherence and partial coherence of CTX and AN, and CTX and PT were computed as described above. Cortex-anterior thalamus (CTX/AN_PT) partial coherence was computed by conditioning on PT. Similarly, cortex-posterior thalamus (CTX/PT_AN) partial coherence was computed by conditioning on anterior thalamus. The *partial-multiple* coherence between cortex and anterior thalamus after removing the effects of posterior thalamus and hippocampus were computed for one of the animals.

4) *Statistical Analysis*: Ordinary coherence, partial coherence, and relative band power were analyzed with two-way analysis of variance (ANOVA). The mixed-model repeated-

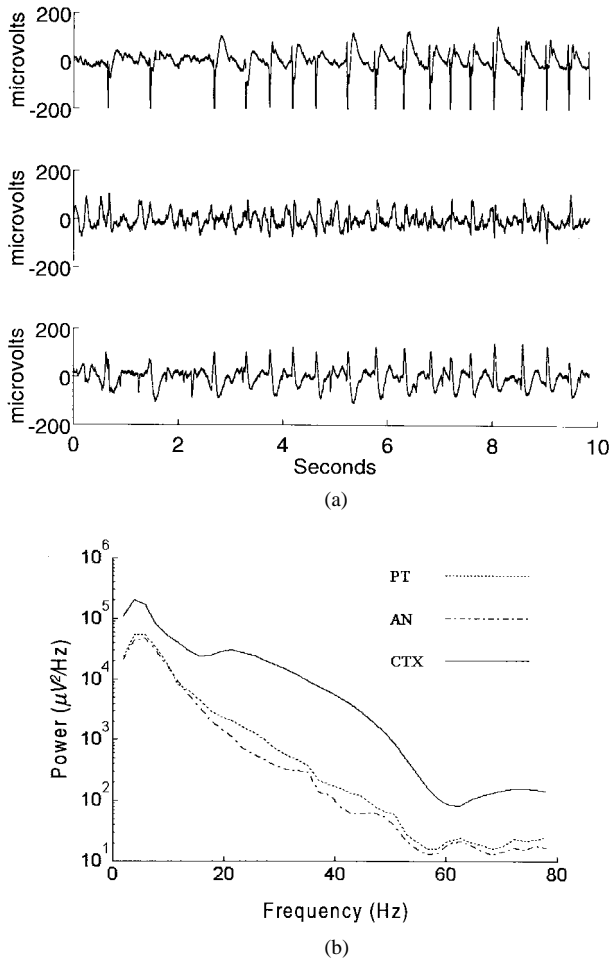


Fig. 2. (a) Representative EEG recorded from (top) CTX, (middle) PT, and (bottom) AN nuclei and (b) their representative power spectra. Legend: Solid-CTX; Plus-PT; and Circles-AN spectral densities.

measures ANOVA method with multiple observations was used [23]. The two factors were seizure interval (SI) X electrode (E). In all cases, factor SI can refer to either *baseline* and *clonic seizure* episodes. Factor E refers to location (electrode derivation). For band power comparisons this refers to single sites, CTX, AN, or PT. In the case of coherence analysis comparisons, the factor E refers to either CTX/AN or CTX/PT. Simultaneous confidence intervals were constructed for these contrasts: i) for relative band power, clonic (summed CTX/AN/PT) versus baseline (summed CTX/AN/PT), CTX versus AN, CTX versus PT, CTX versus subcortical {AN&PT}; ii) for coherence analysis, CTX/AN versus CTX/PT coherence or partial coherence. Ordinary and partial coherence were normalized using Fisher Z transform [14] as

$$z(f) = \tanh^{-1} \gamma^2(f), \quad (16)$$

whereas, relative band power were normalized using the logit transformation [24]

$$z_k = \log\left(\frac{\bar{P}_k}{1 - \bar{P}_k}\right) \quad (17)$$

before analysis.

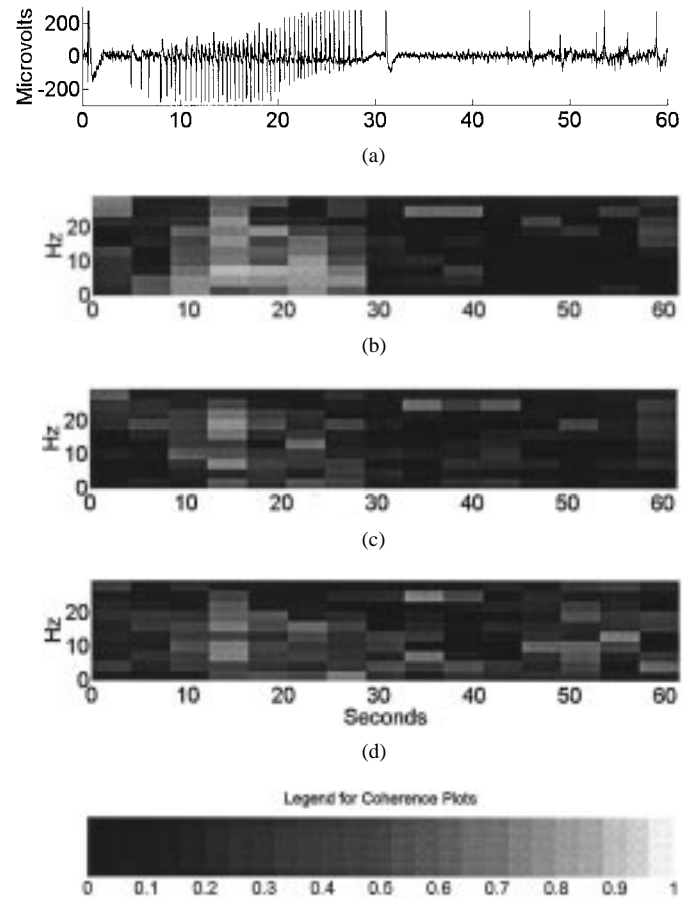


Fig. 3. Progressive changes in coherence during a clonic seizure episode. (a) shows the cortical EEG recording with the same time scale; (b), (c), and (d) show concurrent time-frequency plot showing the course of various ordinary coherences before, during, and after a clonic seizure episode, respectively; Frequency range up to 30 Hz; (b) ordinary coherence between CTX and AN (CTX/AN), (c) the ordinary coherence between CTX/PT during this period; (d) AN/PT coherences across the entire frequency range during a 60-s epoch.

IV. RESULTS

A. Power Distribution

Analysis of power spectral densities reveals distinct spectral differences between anterior thalamus and cortex. Fig. 2 shows a typical clonic seizure EEG and the power spectra of CTX, AN and PT. Although spectral energy is highly concentrated at low frequencies for all derivations, spectral rolloff is considerably steeper in AN than in CTX and PT. Statistical analysis of relative band power shows AN has little relative power in higher frequencies. The 99% confidence interval for the CTX versus AN power contrast is consistently positive for frequency bands above 18 Hz during clonic EEG episodes. significant CTX versus PT contrast exists within any frequency band.

B. Coherence Analysis

Fig. 3(b) shows the progression of the CTX-AN coherence in several bands from preclonic through the clonic seizure stage and culminating in a postictal period for a single PTZ-treated rat. Coherence remains above 0.5 for several frequency bands below 30 Hz during cortical spiking. During these same

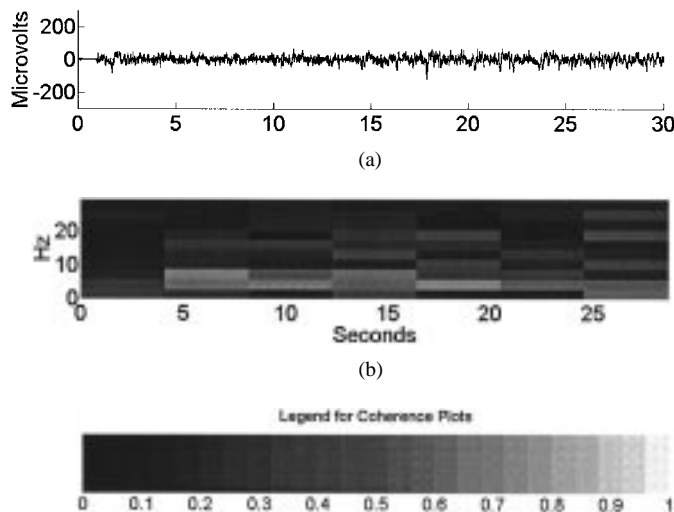


Fig. 4. Time-frequency coherence plot for baseline data before PTZ infusion: (a) the cortical EEG during baseline and (b) AN/PT ordinary coherence. Note that there is strong coherence between AN and PT even before the convulsant agent is given.

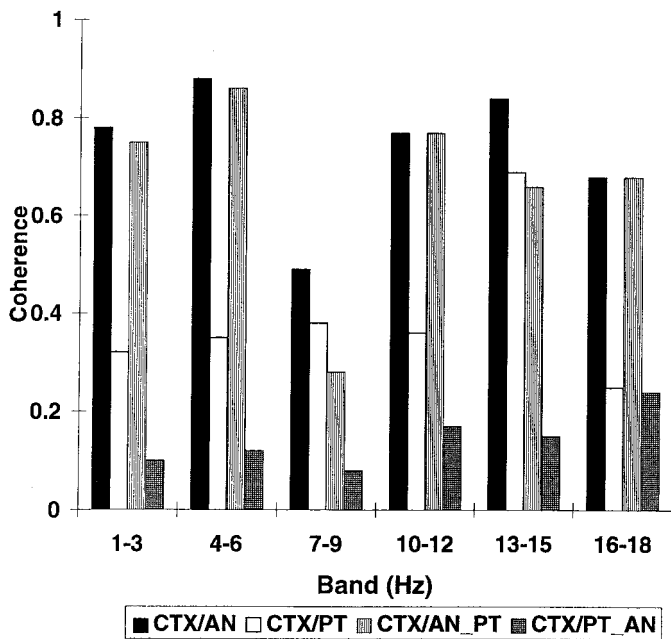


Fig. 5. Comparison of average coherences of across all bands during 8-s clonic seizure episode for a single animal. We exhibit both CTX/AN and CTX/PT ordinary and partial coherences during a seizure. CTX/AN coherence is not greatly diminished when the effects of PT are moved as partial coherence shows. In contrast, partial coherence of CTX/PT with AN removed almost vanishes.

episodes we see an increase in AN/PT coherence [Fig. 3(d)]. This high *subcortical* coherence motivates the use of partial coherence analysis. The largest peaks in this coherence are between 10 Hz and 20 Hz. Low coherence is maintained for frequencies under 6 Hz in both of these cases.

Consideration of large CTX/PT [Fig. 3(c)] and AN/PT [Fig. 3(d)] coherences leads naturally to the inclusion of partial coherence estimation in the analysis procedure. Examination of the coherences during a 30-s baseline episode prior to the infusion of PTZ is shown in Fig. 4. What is particularly

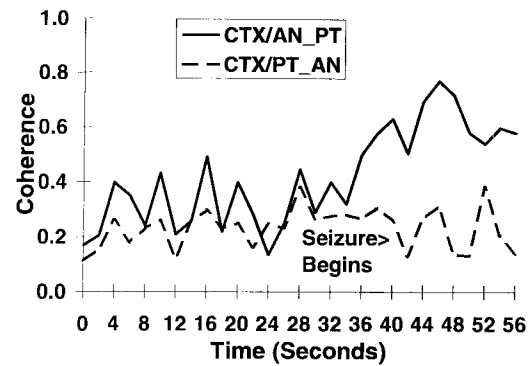


Fig. 6. Comparison of CTX/AN_PT and CTX/PT_AN partial coherence as clonic seizure develops. Data were smoothed with a 5-point triangular window. Note the anticipatory rise in coherence between CTX and AN before the actual clonic seizure begins.

interesting is that AN and PT have large coherences [Fig. 4(b)] over a good portion of the baseline period, even in the absence of clonic seizure activity.

Fig. 5 shows that the partial coherence between CTX and AN is not substantially diminished by conditioning on the activity from the PT. Further analysis of ordinary and partial coherence shows that AN is strongly coherent with CTX during the initial and developed stages of a seizure, especially around the spike repetition frequencies (0–6 Hz). Fig. 6 traces the changes in partial coherence between CTX and AN with PT removed (CTX/AN_PT) leading to a clonic seizure expression. In contrast, the partial coherence CTX/PT is greatly reduced when the linear effects of AN are removed (CTX/PT_AN). A time and frequency plot of partial coherences is shown in Fig. 7. The partial coherence of CTX/AN_PT removed shows a broad range of high coherence frequencies. What is particularly interesting to note is that the coherence of CTX/AN is seemingly larger when HPC is removed in Fig. 7(c). Although HPC is often times considered to be very sensitive for creation and maintenance of seizure activity, removing the HPC does not diminish the coupling between AN and CTX.

Statistical analysis reveals significantly lower *p* values (more significant differences) for the null hypothesis of equality of mean in two-way ANOVA using *ordinary* coherence than partial coherence for the strongest spectral bands (frequencies less than 20 Hz). Using partial coherence, once the opposing channel is removed (AN from CTX/PT and PT from CTX/AN), differences among cases is less robust as seen in Fig. 8. The only frequency band virtually unaffected by partialing out of contaminant channels is the lowest frequency band from 1 to 3 Hz. To underscore this effect the only band showing a positive definite 95% confidence interval for the coherence difference contrasts, (CTX/AN-CTX/PT) ($p < 0.05$), was within the frequency range of 1–3 Hz.

The partial coherence between anterior thalamus and cortex after removing the effects of both hippocampus and posterior thalamus is computed for one of the animals. Comparing the partial coherence of CTX/AN_PT [Fig. 7(a)] to the partial-multiple coherence of CTX/AN with *both posterior thalamic and HPC influences removed* (CTX/AN_PT&HPC) from

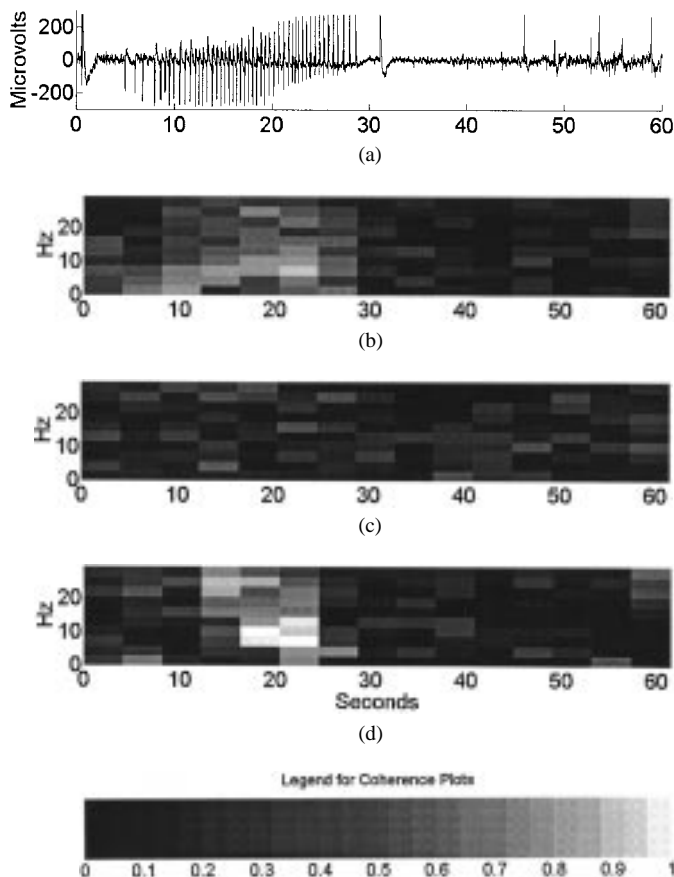


Fig. 7. Time-frequency plots showing partial coherence evolution. Using the same clonic seizure signal (a) as in Fig. 4, we show (b) CTX/AN_PT and (c) CTX/PT_AN partial coherences. The partial coherence of CTX/AN_HPC is also shown (d). Note that even after removing HPC, there is strong coherence between CTX and AN.

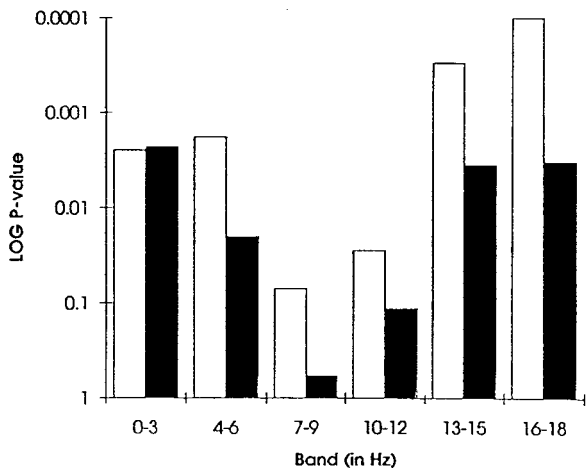


Fig. 8. Plot of p -values for accepting equality of means null hypothesis from two-way ANOVA in comparison of CTX/AN versus CTX/PT coherences. Comparison of p -values for ordinary versus partial coherences. Notice that change in p -value is large for all bands in moving from ordinary to partial coherences. Only the smallest frequency band near the pacing frequency of 1–3 Hz shows the least amount of change. This band is most resistant to the effect of partialing out the opposing channel from CTX/AN and CTX/PT coherences. □: ordinary coherence. ■: partial coherence.

Fig. 9, we see loss of the HPC signal contribution reduces coherence substantially. Later in the clonic seizure episode,

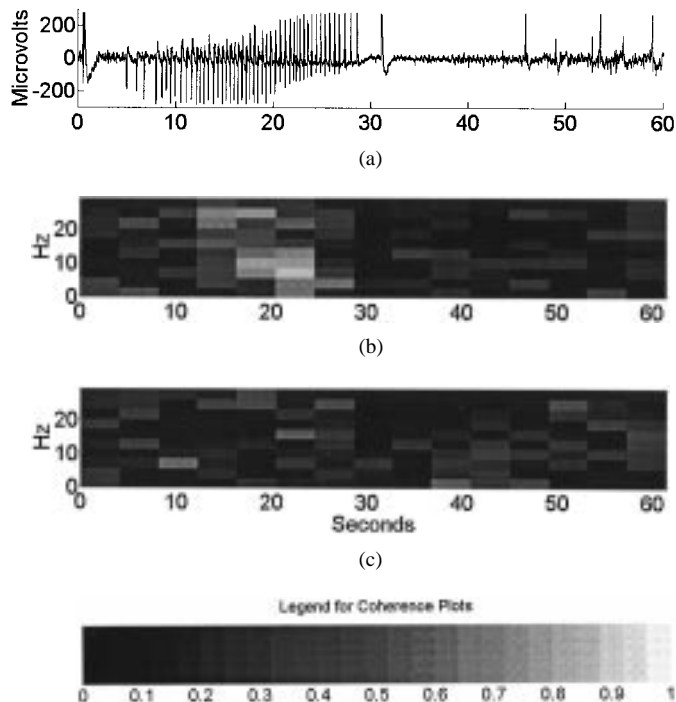


Fig. 9. (a) For the same clonic episode as in Fig. 4, time-frequency plots of (b) CTX/AN coherence after removing posterior thalamic (PT) and HPC influences; (c) CTX/PT coherence after removing AN and HPC effects. Notice the retention of sizable coherence in several frequency bands in CTX/AN_PT&HPC partial-multiple coherence case later in the seizure period.

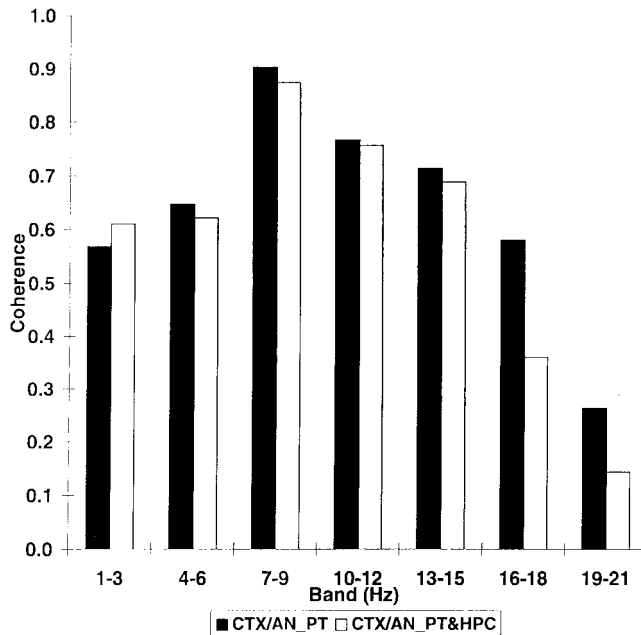


Fig. 10. Comparison of single epoch partial-multiple coherence (CTX/AN_PT&HPC) versus partial coherence (CTX/AN_PT) from of a clonic seizure. Specific CTX/AN_PT&HPC and CTX/AN_PT coherence values chosen are from sixth time epoch from time-frequency plots 9(b) and 7(b), respectively. Note that partial-multiple coherence actually stays close to values from partial coherence in most frequency bands after hippocampus is removed.

however, the time-frequency plot of the partial-multiple coherence shows that a large frequency region between 1 Hz and 30 Hz exhibits high residual coherence. During late periods of

the clonic several frequency components retain their original high coherence even after conditioning on both PT and HPC as shown in a single 4-s epoch of partial-multiple coherence in Fig. 10.

V. DISCUSSION AND CONCLUSIONS

The results described in the Section IV show that AN and CTX interact strongly during epileptic seizures. Despite spectral differences, the coherence between CTX and AN is significantly higher than CTX and the PT at the low frequencies. This finding is significant because high coherence in the 1–3-Hz band corresponds to propagation of strong 3-Hz spike-and-wave pacing rhythm characteristic of PTZ seizures. Likewise the CTX/AN partial coherence does not vanish when the influence of a third channel, PT is included. In contrast, the partial coherence between CTX and PT is greatly diminished after conditioning on AN. In other words, AN explains the observed correlation between CTX and PT in the low frequencies. Gersch *et al.* [10], [11], [15] have proposed an interpretation of causality based on partial coherence: a channel is causal to a pair of channels, if removing its effects causes the partial coherence of the pair to fall to zero. In this sense, AN can be considered to drive CTX and the control at the low frequencies. These results are consistent with previous physiological studies demonstrating the importance of AN in the expression of generalized seizures [6], [7], [25].

It should be pointed out, however, that our method differs from that of Tharp and Gersch [11], as well as Lopes da Silva *et al.* [13]. They focus on determining the residual coherence between a pair of EEG channels after conditioning on a third. Our focus, instead, has been to compare a pair of partial coherences derived from two subcortical centers. Our method relies on the possibility of cross-channel contamination or interference. In order to make the comparison between the AN and the PT, we remove the opposing channel's influence from the ordinary coherences. We compare orthogonal partial coherences by this "cleaning out" of crosstalk between centers. The strength of AN's involvement in the seizure process is affirmed by the magnitude of its residual coherence after the influence of PT is removed and then again after HPC contributions vanish.

This distinction between our method and the Tharp and Gersch [11] procedure is natural since generalized seizures, unlike focal epilepsies, do not originate from a single structure, but rather result from an integrated expression of facilitative and inhibitory influences between cortical and subcortical structures [26]. The expression of a generalized seizure might involve multiple pathways and feedback so causality interpretation could be difficult. The aim of our study is to show that if a subcortical area is involved in seizure expression, it exhibits significantly higher coherence and partial coherence with CTX than other inert areas. The hypothesis that a neuropathway is involved in seizure propagation can, therefore, be tested using coherence and partial coherence. This low-frequency range of high coherences strongly agrees with authors such as [27] as well.

For our study, it is neither necessary nor desirable to compute the partial coherence for all possible combinations of channels. Since PTZ-generalized seizures spread from subcortical to cortical brain, CTX is considered the end-point and, therefore, does not drive the subcortical areas. Naturally, in any study of coherence, multiple coherence, nonlinear effects and noise all have a substantial effect in reducing coherence. In several high-frequency ranges, nonlinear associations may account for coupling that is left undetected when only linear effects are considered [14].

We found that including hippocampus does not reduce the partial coherence between CTX and AN. Hippocampus is a well-known epileptogenic area. The strong coherence of anterior thalamus with CTX, therefore, cannot be explained simply by its association with hippocampus. One resultant hypothesis is that AN, by its anatomical connections with hippocampus, might mediate the transfer of seizure activities to cortex.

In summary, we show that spectral analysis and its by-products, ordinary and partial coherence can identify brain elements important for the propagation of generalized seizures. There is substantial evidence to show that the AN has active involvement during the production of highly synchronous EEG seizure activity. Coherence analysis of epileptic EEG can, therefore, aid in our understanding of seizure propagation and its generalization.

ACKNOWLEDGMENT

The authors would like to recognize A. Kolandaivelu and E. Lancaster for kind and generous programming support.

REFERENCES

- [1] R. S. Fisher, "Animal models of the epilepsies," *Brain Res. Rev.*, vol. 14, pp. 245–278, 1989.
- [2] E. R. Kandel and J. H. Schwartz, *Principles of Neural Science*. New York: Elsevier, 1985.
- [3] M. A. Mirski, "Unraveling the neuroanatomy of epilepsy," *Amer. J. Neuroradiol.*, vol. 14, pp. 1336–1342, 1993.
- [4] M. A. Mirski and R. S. Fisher, "Electrical stimulation of the mammillary nuclei raises seizure threshold to pentylenetetrazol in rats," *Epilepsia*, submitted for publication.
- [5] M. A. Mirski and J. A. Ferrendelli, "Interruption of the connections of the mamillary bodies protect against generalized pentylenetetrazol seizures in guinea pigs," *J. Neurosci.*, vol. 7, pp. 662–670, 1987.
- [6] ———, "Interruption of the mammillothalamic tracts prevents seizures in guinea pigs," *Sci.*, vol. 226, pp. 72–74, 1984.
- [7] ———, "Selective metabolic activation of the mamillary bodies and their connections during ethosuximide-induced suppression of pentylenetetrazol seizures," *Epilepsia*, vol. 51, pp. 194–203, 1985.
- [8] D. O. Walter and W. R. Adey, "Analysis of brain-wave generators as multiple statistical time series," *IEEE Trans. Biomed. Eng.*, vol. BME-12, pp. 8–13, 1965.
- [9] M. A. B. Brazier, "Spread of seizure discharges in epilepsy: Anatomical and electrophysiological considerations," *Exp. Neurol.*, vol. 36, pp. 263–272, 1972.
- [10] W. Gersch and G. V. Goddard, "Epileptic focus location: Spectral analysis method," *Sci.*, vol. 169, pp. 701–702, 1970.
- [11] B. R. Tharp and W. Gersch, "Spectral analysis of seizures in humans," *Comput. Biomed. Res.*, vol. 8, pp. 503–521, 1975.
- [12] D. M. Tucker, D. L. Roth, and T. B. Bair, "Functional connections among cortical regions: topography of EEG coherence," *Electroencephal. Clin. Neurophysiol.*, vol. 63, pp. 242–250, 1986.
- [13] F. H. Lopes da Silva, J. E. Vos, J. Mooibroek, and A. Van Rotterdam, "Relative contributions of intracortical and thalamo-cortical processes in the generation of alpha rhythms, revealed by partial coherence analysis," *Electroencephal. Clin. Neurophysiol.*, vol. 50, pp. 449–456, 1980.

- [14] J. S. Bendat and A. G. Piersol, *Random Data: Analysis and Measurement Procedures*. New York: Wiley, 1986.
- [15] W. Gersch, "Causality or driving in electrophysiological signal analysis," *Math. Biosci.*, vol. 14, pp. 177-196, 1972.
- [16] T. F. Dagi and C. E. Poletti, "Reformulation of the papez circuit: Absence of hippocampal influence on cingulate cortex unit activity in the primate," *Brain Res*, vol. 259, pp. 229-236, 1983.
- [17] V. B. Domesick, "Projections from the cingulate cortex in the rat," *Brain Res*, vol. 12, pp. 296-320, 1969.
- [18] C. D. Yingling and J. E. Skinner, "Regulation of unit activity in nucleus reticularis thalami by the mesencephalic reticular formation and the frontal granular cortex," *Neurophysiol. Clin.*, vol. 39, 1975.
- [19] D. Pare, M. Steriade, M. Deschenes, and G. Oakson, "Physiological characteristics of anterior thalamic nuclei, a group devoid of inputs from reticular thalamic nuclei," *J. Neurophysiol.*, vol. 57, pp. 1669-1685, 1987.
- [20] D. Brillinger, *Time Series: Data Analysis and Theory*. San Francisco, CA: Holden-Day, 1981.
- [21] R. J. Racine, "Modification of seizure activity by electrical stimulation; motor seizures," *Electroencephal. Clin. Neurophysiol.*, vol. 32, pp. 281, 1972.
- [22] P. D. Welch, "The use of the fast Fourier transform for the estimation of power spectra," *IEEE Trans. Audio Electroacoust.*, vol. AE-15, pp. 70-73, 1970.
- [23] D. F. Morrison, *Multivariate Statistical Methods*, 3rd. ed. New York: McGraw-Hill, 1990.
- [24] T. Gasser, P. Bacher, and J. Mocks, "Transformation toward the normal distribution of broad band spectral parameters of the EEG," *Electroencephal. Clin. Neurophysiol.*, vol. 53, pp. 119-124, 1981.
- [25] M. A. Mirski and J. A. Ferrendelli, "Anterior thalamic mediation of generalized pentylene-tetrazol seizures," *Brain Res*, vol. 399, pp. 212-223, 1986.
- [26] P. Gloor, "Generalized cortico-reticular epilepsies: Some considerations on the pathophysiology of generalized bilaterally synchronous spike and wave discharge," *Epilepsia*, vol. 9, pp. 249-263, 1968.
- [27] H. P. Zaveri, "Generation and propagation of seizures in temporal lobe epilepsy," Ph.D. dissertation, Bioengineering Department, Univ. Michigan, Ann Arbor, 1993.



David Lee Sherman (S'83-M'93) was born on August 31, 1957 in Buffalo, NY. He received the A.B. degree in psychology from Columbia University, New York, NY, in 1980; the B.S. degree in electrical engineering from Florida Atlantic University, Boca Raton, FL, in 1983; and the M.S. and Ph.D. degrees from Purdue University, West Lafayette, IN, both in electrical engineering.

He received a Whitaker Postdoctoral Fellowship in 1993 and a McDonnell-Pew Fellowship in Cognitive Neuroscience in 1995 for research at the Johns

Hopkins University, Baltimore, MD., where he is currently a Research Associate in the Department of Biomedical Engineering. His research interests include neuroelectric signal analysis and higher-order spectral analysis.



Yien Che Tsai was born in Saigon in 1971 and grew up in Singapore. He graduated with a double major in biomedical engineering and electrical engineering from the Johns Hopkins University, Baltimore, MD, in 1996. He is currently working toward the Ph.D. degree in biomedical engineering at the Johns Hopkins University.

His research interests are neuroscience, imaging and signal processing.

Mr. Tsai received the Provost's Research Award for 1995 and the Richard Johns Award for biomedical engineering in 1996.

Lisa Ann Rossell, photograph and biography not available at the time of publication.



Marek A. Mirski received the B.S. degree (chemistry and biology) from the Massachusetts Institute of Technology, Cambridge. He subsequently completed the combined M.D./Ph.D. program at Washington University, St. Louis, MO, in 1986. The Ph.D. degree work was in the Department of Neuroscience, in the field of Epilepsy Research, on the topic "Functional anatomy of pentylene-tetrazol seizures." He continued the postgraduate medical education at Johns Hopkins Hospital, Baltimore, MD, where he completed residency programs in

both neurology and anesthesiology. His subspecialty training included clinical fellowships in both neuroanesthesiology and neurological critical care.

He was on the faculty at Johns Hopkins University from 1991-1995 as an Assistant Professor in Anesthesiology and Critical Care Medicine with additional appointments in Neurology and Neurosurgery. He is now the Medical Director of the Neuroscience Institute, Queen's Medical Center, Honolulu, HI, and an Associate Professor of Medicine and Surgery, University of Hawaii, Manoa, HI. He is also affiliated with the Department of Neuroanesthesia and Neurological Critical Care.

Nitish V. Thakor (S'78-M'81-SM'89-F'97), for a photograph and biography, see p. 356 of the May 1997 issue of this TRANSACTIONS.